λ-*ECLIPSE*: Multi-Concept Personalized Text-to-Image Diffusion Models by Leveraging CLIP Latent Space

Maitreya Patel[*†] **Sangmin Jung**[*] **Chitta Baral** **Yezhou Yang**
Arizona State University
https://eclipse-t2i.github.io/Lambda-ECLIPSE/

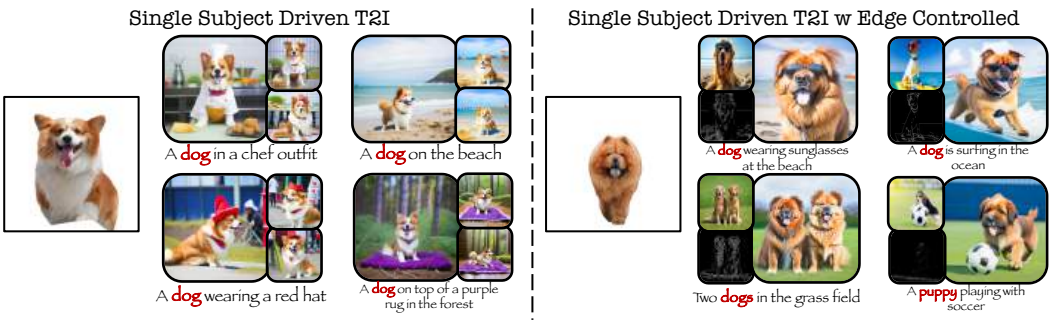

Figure 1: λ-*ECLIPSE* can estimate subject-specific image embeddings while maintaining the balance between concept and composition alignment in a resource-efficient way.

Abstract

Despite the recent advances in personalized text-to-image (P-T2I) generative models, it remains challenging to perform finetuning-free multi-subject-driven T2I in a resource-efficient manner. Predominantly, contemporary approaches, involving the training of Hypernetworks and Multimodal Large Language Models (MLLMs), require heavy computing resources that range from 600 to 12300 GPU hours of training. These subject-driven T2I methods hinge on Latent Diffusion Models (LDMs), which facilitate T2I mapping through cross-attention layers. While LDMs offer distinct advantages, P-T2I methods' reliance on the latent space of these diffusion models significantly escalates resource demands, leading to inconsistent results and necessitating numerous iterations for a single desired image. In this paper, we present λ-*ECLIPSE*, an alternative prior-training strategy that works in the latent space of a pre-trained CLIP model without relying on the diffusion UNet models. λ-*ECLIPSE* leverages the image-text interleaved pre-training for fast and effective multi-subject-driven P-T2I. Through extensive experiments, we establish

* indicates equal contribution, † corresponding author: maitreya.patel@asu.edu

Preprint.

that λ-*ECLIPSE* surpasses existing baselines in composition alignment while preserving concept alignment performance, even with significantly lower resource utilization. λ-*ECLIPSE* performs multi-subject driven P-T2I with just 34M parameters and is trained on a mere 74 GPU hours. Additionally, λ-*ECLIPSE* demonstrates the unique ability to perform multi-concept interpolations.

1 Introduction

The field of text-to-image (T2I) diffusion models has recently witnessed remarkable advancements, achieving greater photorealism and enhanced adherence to textual prompts. This has catalyzed the emergence of diverse applications, notably subject-driven personalized T2I (P-T2I) models. In particular, this encompasses the intricate task of learning and reproducing novel visual concepts or subjects in varied contexts requiring high concept and compositional alignment. The complexity escalates further when multi-subject personalization is desired.

Early works employed concept-specific optimization strategies involving fine-tuning certain parameters within T2I diffusion models [11, 39, 20, 48, 12]. Although these methods achieve state-of-the-art (SOTA) performance, they struggle with generalization and are time-intensive. Contemporary research is pivoting towards fast personalization techniques. Within this paradigm, there are two types of popular approaches: 1) Methods that involve training hypernetworks and integrating new layers or parameters within pre-trained diffusion UNet models [50, 52, 47, 43, 40], and 2) MLLM-based learning of prior models that focuses on leveraging text-latent space of frozen diffusion UNet model [30, 46].

The hypernetwork-based strategy achieves single-concept customization but has not been extended to multi-concepts. Moreover, when combined with additional control (i.e. Canny edge map), they struggle to maintain the concept alignment ($\sim$30% drop in performance; Section 4) and strongly favor the edge map. At the same time, MLLM-based approaches can perform fast multi-concept customization but require heavy computing resources. In Table 1, we provide the overview of various single and multi-concept customization methodologies in terms of total parameters, iterations, and GPU hours required to train the models. It can be observed that multi-concept customization methodologies further increase the resource requirements. For instance, Kosmos-G [30] consumes 18x more resources than IP-Adapter [52]. And Emu2 [46] requires training of 19x more parameters compared to Kosmos-G. Hence, despite MLLMs' seemingly useful scenarios it is not viable to blindly train them. Therefore, in this work, we focus on answering one question: `What are the alternative methodology and design choices we can make to improve resource efficiency?`

Upon further investigation, we find that most subject-driven T2I approaches build upon variants of the Latent Diffusion Model (LDM) [38], specifically Stable Diffusion models. These LDMs employ cross-attention layers to condition diffusion models with text embeddings, necessitating a mapping of target subject images to latent spaces compatible with the diffusion models at the prior training stage. This is also known as score distillation instruction tuning for MLLMs [30]. As there is no choice but to learn this text-to-image diffusion latent space, it involves backpropagation through the entire diffusion model often comprising over a billion parameters, contributing to the inefficiency of existing P-T2I methods.

To improve the resource efficiency for multi-concept image generation, we present λ-*ECLIPSE*[1], which leverages the properties of UnCLIP T2I models (e.g. DALL-E 2 [35] and Kandinsky v2.2 [37]) and performs P-T2I in the compressed latent space. Specifically, unlike previous MLLM-based methodologies, λ-*ECLIPSE* aligns the output space of priors with CLIP vision space instead of the CLIP text space. λ-*ECLIPSE* takes multiple images and text instructions as input and estimates the respective vision embeddings, which can be used by the frozen diffusion UNet model from the UnCLIP stack to generate the resulting image. This elevates the training time dependencies on diffusion models for P-T2I; significantly contributing to the resource efficiency. Additionally, as diffusion or MLLM-based priors are still compute heavy due to a huge number of parameters and slower convergence, we build upon *ECLIPSE* [32] and SEED [13], which shows that text-to-image

[1]The designation λ-*ECLIPSE* is inspired by its conceptual alignment with the λ-calculus. In this context, the λ-*ECLIPSE* model functions similarly to a functional abstraction within λ-calculus, where it effectively binds variables. These variables, in our case, represent novel visual concepts that are integrated through composition prompts. Here, *ECLIPSE* indicates our architecture design choice.

Table 1: **A quick overview of previous works on P-T2I.** Our method is the first to offer multi-concept-driven generation without depending on diffusion UNet models (except for inference). We provide the extended overview table in the appendix.

Method	Multi Concepts	Finetuning Free	Diffusion Free	Total opt. params	Training Steps	Dataset Size	GPU Hours
Textual Inversion [11]	✗	✗	✗	768	5000	-	1
DreamBooth [39]	✗	✗	✗	0.9B	800	-	0.2
ELITE [50]	✗	✓	✗	77M	135K	125K	336
BLIP-Diffusion [22]	✗	✓	✗	1.5B	500K	129M	2304
IP-Adapter [52]	✗	✓	✗	22M	1M	-	672
Custom Diffusion [20]	✓	✗	✗	57M	500	-	0.1
Subject-Diffusion [28]	✓	✓	✗	252M	300K	76M	-
Kosmos-G [30]	✓	✓	✗	1.9B	800K	200M	12300
Emu-2 [46]	✓	✓	✗	37B	70K	162M	-
λ-*ECLIPSE* **(ours)**	✓	✓	✓	34M	100K	2M	74

mapping can be optimized through contrastive pre-training. Here, we select *ECLIPSE* as preferred choice of prior architecture for best efficiency. At last, we propose a subject-driven instruction tuning task based on the image-text interleaved data as a pre-training strategy. This involves creating 2 million high-quality image-text pairs, where text embeddings linked to subjects are substituted with the respective image embeddings, which in return are considered as input to the λ-*ECLIPSE*. While λ-*ECLIPSE* can be plugged with these pre-trained methods, we explore the possibility of λ-*ECLIPSE* to incorporate Canny edge as an additional control to synergetically work with subject-driven image generation tasks. Figure 1 provides the overview of λ-*ECLIPSE* capabilities.

Overall, we propose λ-*ECLIPSE* as an initial attempt to motivate future works on designing resource-efficient solutions for MLLM-based approaches. We summarize our main contributions as follows: 1) We introduce a training-time diffusion-independent, UnCLIP-based prior learning strategy for enabling efficient and fast multi-subject customization. 2) Extensive experiments on Dreambench, Multibench, and ConceptBed reveal that λ-*ECLIPSE* (34M parameter model) trained on a mere 74 GPU hours can achieve competitive performance to that of big counterparts (having 2B-37B parameters) and improve text-composition alignment. 3) At last, λ-*ECLIPSE* inherits the smooth CLIP latent space. This allows us to perform the seamless transition between multi-concept generated images.

2 Related Works

Text-to-Image Generative Models. Pioneering efforts in image generation, notably DALL-E [36] and CogView [10], leveraged autoregressive models to achieve significant results. Recent advancements predominantly feature diffusion models, acclaimed for their high image fidelity and diversity in text-to-image (T2I) generation. A notable example is Stable Diffusion, which builds upon the Latent Diffusion Model (LDM) [38] and excels in semantic and conceptual understanding by transitioning training to latent space. Imagen [41], Pixart-α [7], and DALL-E 3 [5] propose using a large T5 language model to improve language understanding. DALL-E 2 [35] along with its UnCLIP variation models such as Kandinsky [37] and Karlo [21], uses a diffusion prior and diffusion UNet modules to generate images using the pre-trained CLIP [34] model.

Personalized T2I Methods. Approaches like Textual Inversion [11], DreamBooth [39], and Custom Diffusion [20] focus on training specific parameters to encapsulate visual concepts. LoRA [16] and Perfusion [47] target efficient fine-tuning adjustments, particularly rank 1 modifications. However, these methods are constrained by their requirement for concept-specific tuning. ELITE [50] was the first approach addressing fast customized generation for single-subject T2I. BLIP-Diffusion [22] adapts the BLIP2 encoder [23], training approximately 1.5B parameters to enable zero-shot, subject-driven image generation. IP-Adapter introduces a decoupled cross-attention mechanism, negating the need to train the foundational UNet model by permitting fine-tuning of a reduced number of 22M parameters.

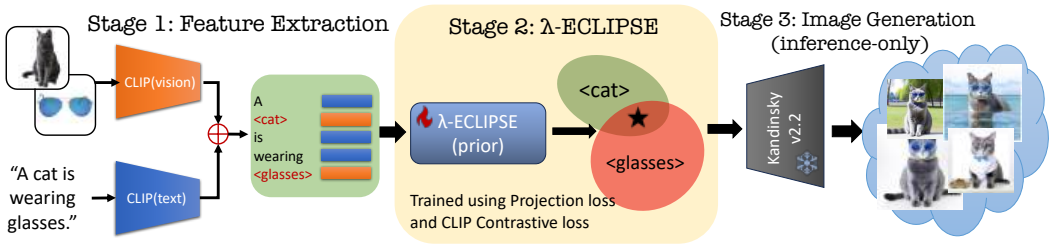

Figure 2: **This figure illustrates the three stages of the λ-*ECLIPSE* pipeline.** 1) Create the image-text interleaved features using frozen CLIP. 2) Pre-train the λ-*ECLIPSE* (34M parameters) using Eq. 1, which ensures the mapping to the desired latent space given the image-text interleaved data. 3) During inference, the frozen Kandinsky v2.2 diffusion UNet model takes the output from the λ-*ECLIPSE* and generates the image.

Mix-of-Show [14] and Zip-LoRA [43] train individual concepts and then combine them to generate multiple subjects. Break-A-Scene [4] shows multi-concept capability but requires single images containing diverse objects. Subject Diffusion [28] creates a high-quality dataset and presents the precision control for fast personalized multi-subject image generation. Kosmos-G and Emu2 [46], akin to Subject-Diffusion [28], employs a Multimodal Large Language Model (MLLM) for text-image embedding alignment, though it necessitates extensive parameter optimization (1.9B-37B). These multi-subject P-T2I methods are not only demanding in terms of parameters but also depend on a massive number of frozen parameters of the diffusion UNet model, increasing training computational loads. In contrast, our model, λ-*ECLIPSE*, forgoes test-time fine-tuning and training-time reliance on the diffusion UNet model for single and multi-concept, control-guided P-T2I, positioning it as a resource-efficient solution.

At last, methods like GLIGEN [24], ControlNet [53], and UniControl [33] incorporate additional controls (i.e., edge map, depth, segmentations) into the diffusion model to generate the desired images. BLIP-Diffusion, IP-Adapter, and Kosmos-G can leverage such pre-trained controls. However, in many scenarios, these controls are too strong, making generated images lose subject-specific details. We show that λ-*ECLIPSE* learns to balance the edge map, subjects, and composition. We offer a more comprehensive review of related works in the appendix.

3 Method

In this section, we introduce λ-*ECLIPSE*, our approach to multi-subject personalized text-to-image generation. Our method combines the contrastive text-to-image strategy from *ECLIPSE* with the novel image-text interleaved pretraining strategy, notably omitting the need for explicit diffusion modeling. Our approach mainly capitalizes on the efficient utilization of the CLIP latent space. Figure 2 outlines the end-to-end framework.

The primary objective of λ-*ECLIPSE* is to facilitate single and multi-subject P-T2I generation processes, accommodating edge maps as conditional guidance. Initially, we detail the problem formulation and elaborate on the UnCLIP stack design of the λ-*ECLIPSE*. Subsequently, we delve into the image-text interleaved training methodology. This fine-tuning process enables the λ-*ECLIPSE* to harness semantic correlations between CLIP image and text latent spaces while preserving subject-specific visual features.

3.1 Text-to-Image Prior Mapping

In the UnCLIP T2I models, the objective of the text-to-image prior model (f_θ) is to establish a proficient text-to-image embedding mapping. This model is designed to adeptly map textual representations to their corresponding visual embeddings, denoted as ($f_\theta : z_y \rightarrow z_x$), where $z_{x/y}$ represent the embeddings for images and text, respectively. The visual embedding predictions ($\hat{z_x} = f_\theta(z_y)$) are then effectively utilized by the diffusion image generators (h_ϕ), which are inherently conditioned on these vision embeddings ($h_\phi : z_x \rightarrow x$). In our experiments, we utilize the Kandinsky v2.2 diffusion UNet model as h_ϕ.

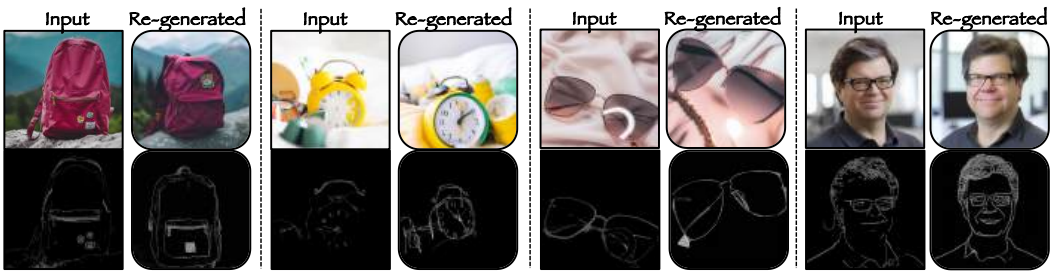

Figure 3: **CLIP(vision) features capture the semantics and fine-grained visual details.** Each input is given as input to the Kandinsky v2.2 and re-generated from the decoder. (Top: Real-images, Bottom: Canny edge)

As shown in Figure 3, the CLIP vision encoder preserves the necessary features in z_x required to reconstruct the input image and achieves a similar concept alignment score (`DINO: 0.66`) as finetuning-based DreamBooth method [39].

Our goal is to accurately estimate the image embedding $\hat{z}_x$, incorporating the subject representations, thereby eliminating reliance on h_ϕ during training. Existing LDM-based P-T2I methods are limited by the LDM's singular module approach ($h_\phi : z_y \rightarrow x$). Consequently, mastering the latent space of h_ϕ becomes essential for effective P-T2I for the baseline methodologies, which limits the previous methodologies.

We propose a new mapping function, f_θ, which processes text representations (z_y) alongside subject (x_k) specific visual representations (z_{x_k}), to derive an image embedding that encapsulates both text prompts and subject visuals ($\hat{z}_x$). The challenge lies in harmonizing z_{x_k} and z_y within $f_\theta : (z_y, z_{x_k}) \rightarrow \hat{z}_x$, ensuring alignment while preventing overemphasis on either aspect, as this could compromise composition alignment. To address this, we employ the contrastive pre-training strategy after [32]:

$$\mathcal{L}_{prior} = \mathop{\mathbb{E}}_{\substack{\epsilon\sim\mathcal{N}(0,I) \\ z_y, z_{x_k}}} \left[||z_x - f_\theta(\epsilon, z_y, z_{x_k})||_2^2 \right] - \frac{\lambda}{N} \sum_{i=0}^{N} \log \frac{\exp(\langle \hat{z}_x^i, z_y^i \rangle / \tau)}{\sum_{j\in[N]} \exp(\langle \hat{z}_x^i, z_y^j \rangle / \tau)}. \tag{1}$$

Here, λ serves as the hyperparameter. i and j represent the index of the given input batch with the size N. $\langle \cdot \rangle$ represents the inner-product and τ is the temperature parameter. The first loss term (projection loss) measures the mean-squared error between the estimated and actual image embeddings, primarily ensuring concept alignment. However, our preliminary studies reveal that exclusive reliance on this term diminishes composition alignment. Therefore, we stick with the contrastive loss component (the second loss term) to bolster compositional generalization, with λ balancing concept and composition alignment.

Additional Control-based T2I Prior Mapping. Acknowledging the limitations in existing methods, which necessitate learning the diffusion latent space even for additional control inputs, we endeavor to achieve a more nuanced balance between subject, text, and supplementary conditions. Consequently, we have augmented λ-*ECLIPSE* to accommodate an additional modality, a Canny edge map, providing more refined control over subject-driven image generation. This entails modifying the prior model to accept additional conditions ($f'_\theta : (z_y, z_{x_i}, z_c) \rightarrow \hat{z}_x$, here z_c symbolizes the additional modality embedding).

During training, we drop z_c for 1% to improve the unconditional generations. This enhances the stability and broadens the generalization capabilities of λ-*ECLIPSE*, yielding benefits even in the absence of these controls during inference. Our results demonstrate that λ-*ECLIPSE* learns a unified mapping function, accurately estimating target image representations through the effective integration of text, image, and edge maps.

Figure 4: **This figure illustrates a qualitative comparison of λ-*ECLIPSE* with contemporary approaches for single-subject T2I generations, utilizing concepts and prompts from the Dreambench dataset.** For each method, concept, and prompt, we generate four images and select the one that most accurately represents the queried concept and composition.

3.2 Image-text Interleaved Training

Our approach targets developing a versatile prior model capable of processing diverse inputs to estimate target visual outputs. Drawing from earlier methodologies, a straightforward solution involves concatenating different inputs, like combining text ("a dog wearing sunglasses") with respective concept-specific images. Preliminary experiments indicated that this method does not effectively capture the intricate relationships between target text tokens (e.g. "dog") and the corresponding concept images, especially when multiple concepts are present.

To address this, we adopt the interleaved pre-training strategy used in Kosmos-G, but with a notable modification to enhance resource efficiency. We incorporate pretrained frozen CLIP text and vision encoders for extracting modality-specific embeddings—separating text-only from subject-specific images. The key refinement in our process is the substitution of subject token-specific text embeddings with corresponding vision embeddings instead of introducing additional trainable tokens to handle the image embeddings via resampler [2]. First, we extract reference concept visual features ($z_{x_k} \in \mathcal{R}^{1\text{x}1280}$) from the CLIP vision encoder. Similarly, we also extract the text prompt features ($z_y \in \mathcal{R}^{77\text{x}1280}$) from the last layer of the CLIP text encoder. Here, 1280 is the CLIP-specific feature dimension. At last, we replace the concept noun corresponding latent features from z_y with z_{x_k}; resulting in image-text interleaved features while preserving the contextual information of the text features. This alteration allows us to bypass the need to train the big priors models (e.g. MLLMs), significantly improving the model's proficiency in handling interleaved data.

For the generation of high-quality training datasets, we carefully selected 2 million high-quality images from the LAION dataset [42], each with a resolution of 1024x1024. Utilizing BLIP2, we generate captions for these images and employ SAM [19] for extracting noun or subject-specific segmentation masks. Given the CLIP model's requirement for 224x224 resolution images, we avoid resizing the masks within their original resolutions. Instead, we opt for cropping the area of interest using Grounding DINO [25], followed by resizing the masked object while preserving its aspect ratio. This technique is crucial in retaining maximum visual information for each subject during the training phase. We provide more details about the filters used in the supplementary material.

3.3 Additional Finetuning

Due to the nature of UnCLIP models, even if λ-*ECLIPSE* is very accurate, the diffusion UNet model (h_ϕ) may not be effective in generating very unique visual representations. However, such behavior is common across the fast P-T2I methods and they lack in terms of maintaining performance compared to the finetuning-based methods (as outlined in Table 2). Therefore, we extend the λ-*ECLIPSE* and perform concept-specific finetuning.

Compared to the traditional finetuning methodologies (such as DreamBooth), λ-*ECLIPSE* provides very unique advantages. As λ-*ECLIPSE* prior model (f_θ) is pre-trained for personalization, there is no need for further finetuning the f_θ and we need to only finetune diffusion UNet model. Importantly, the fine-tuning of the h_ϕ does not depend on the text embeddings (z_y). Hence, this leads to stable fine-tuning of the h_ϕ; unlike DreamBooth on stable diffusion that observes catastrophic forgetting (Section D). The new fine-tuning objective is:

$$\mathcal{L}_{decoder} = \mathop{\mathbb{E}}_{\substack{\epsilon\sim N(0,I) \\ t\sim[0,T],(z_x)}} \Big[||\epsilon - h_\phi(x^{(t)}, t, z_x)||_2^2 \Big]. \tag{2}$$

Here, z_x is the visual feature of the reference concept image x. Notably, we do not need to use regularization from the DreamBooth as text alignment is already ensured during the pretraining stage of λ-*ECLIPSE*. Moreover, this finetuning can be performed across the set of given visual concepts altogether in a single model without degrading performance.

In summary, the prior model, trained with our image-text interleaved data and supplementary condition, presents an efficient pathway for resource-efficient multi-subject-driven image generations.

4 Experiments

In this section, we first introduce the experimental and evaluation setups. Later, we delve into the qualitative and quantitative results.

Training and inference details. We initialize our model, λ-*ECLIPSE*, equipped with 34M parameters. We train our model on an image-text interleaved dataset of 2M instances, partitioned into 1.6M for training and 0.4M for validation. The model is specifically tuned for the Kandinsky v2.2 diffusion image decoder. Therefore, we use pre-trained OpenCLIP-ViT-G/14[2] as the text and vision encoders, ensuring alignment with Kandinsky v2.2 image embeddings. Training is executed on 2 x A100 GPUs, leveraging a per-GPU batch size of 512 and a peak learning rate of 0.00005, across approximately 100,000 iterations, summing up to 74 GPU hours. During inference, the model employs 50 DDIM steps and 7.5 classifier-free guidance for the Kandinsky v2.2 diffusion image generator. Adhering to baseline methodologies, we perform the P-T2I following the baseline papers' protocols. For λ-*ECLIPSE*, target subject pixel regions in reference images are segmented before embedding extraction via the CLIP(vision) encoder. We drop the Canny edge map during inference unless specified explicitly. Unless specified all results (quantitative and qualitative) are without concept-specific additional fine-tuning.

Evaluation setup. We primarily utilize Dreambench (encompassing 30 unique concepts with 25 prompts per concept) for qualitative and quantitative evaluations using DINO and CLIP-based metrics [39]. Due to their limitations, we extend our evaluations on the ConceptBed [31] benchmark

[2] https://huggingface.co/laion/CLIP-ViT-g-14-laion2B-s12B-b42K

Table 2: **Quantitative comparisons of different methodologies on Dreambench.** The **Bold** and underline represent the metric-specific first and second-ranked methods, respectively. * represents that we re-benchmark the performance from open-source weights.

Method	Base Model	Params	GPU Hours	DINO (↑)	CLIP-I (↑)	CLIP-T (↑)
Textual Inversion	SDv1.5	768	1	0.569	0.780	0.255
DreamBooth	SDv1.5	0.9B	0.2	0.668	0.803	**0.305**
Custom Diffusion	SDv1.5	57M	0.2	0.643	0.790	**0.305**
BLIP-Diffusion	SDv1.5	0.9B	0.1	0.670	**0.805**	0.302
*λ-ECLIPSE**	Kv2.2	0.9B	0.2	**0.682**	0.796	0.304
Re-Imagen	Imagen	-	-	0.600	0.740	0.270
ELITE	SDv1.4	77M	336	0.621	0.771	**0.293**
Subject-Diffusion	SDv1.5	252M	-	**0.711**	0.787	**0.293**
BLIP-Diffusion*	SDv1.5	1.5B	2304	0.603	0.793	0.291
IP-Adapter*	SDv1.5	22M	672	0.629	**0.827**	0.264
IP-Adapter*	SDXL	22M	672	0.613	0.810	0.292
Kosmos-G*	SDv1.5	1.9B	12300	**0.618**	**0.822**	0.250
Emu2*	SDXL	37B	-	0.563	0.765	0.273
*λ-ECLIPSE**	Kv2.2	**34M**	**74**	0.613	0.783	**0.307**

Table 3: **Quantitative comparisons of different methodologies on ConceptBed.** We present results on CCD (↓) across three evaluation categories. The **Bold** and underline represent the metric-specific first and second-ranked methods, respectively. * represents our benchmarking.

Method	Base Model	Concept Replication (↓)	Concept Alignment (↓)	Composition Alignment (↓)
Textual Inversion	SDv1.4	**0.0662**	**0.1163**	0.1436
Dreambooth	SDv1.4	0.0880	0.3551	0.0360
Custom Diffusion	SDv1.4	0.2309	0.4882	**0.0204**
ELITE*	SDv1.4	0.3195	0.4666	0.1832
BLIP-DIffusion*	SDv1.5	0.3510	**0.3245**	0.1589
IP-Adapter*	SDXL	0.3665	0.3571	0.0641
*λ-ECLIPSE**	Kv2.2	**0.2853**	0.3619	**-0.0200**

(covering 80 diverse imagenet concepts and a total of 33K composite prompts), where we report performance on concept replication, concept, and composition alignment using the Concept Confidence Deviation (CCD) metric [31]. We extend Dreambench for multi-subject customization and present the Multibench dataset. Multibench contains about 24 unique concepts and 15 diverse prompts that result in 904 two-subject specific prompts and 1476 three-subject specific prompts. We provide further details about the Multibench in supplementary materials.

4.1 Results & Analysis

Quantitative comparison. The quantitative assessments detailed in Table 2 and Table 3 focus on the single-concept T2I task, while Table 4 shows the results on multi-concept-driven image generation. For Dreambench and Multibench, we generate and evaluate four images per prompt, reporting average performance on three metrics (DINO, CLIP-I, and CLIP-T). In the case of ConceptBed, we process each of the 33K prompts to generate a single concept image. The results, as depicted in these tables, highlight *λ-ECLIPSE*'s superior performance in composition alignment while maintaining competitive concept alignment. Analysis on ConceptBed (Table 3) indicates that *λ-ECLIPSE* exhibits a notable proficiency in concept replication, albeit with a marginal trade-off in concept alignment for enhanced composition fidelity. Comparatively, all baselines prioritize concept alignment, often at the expense of composition alignment. While *λ-ECLIPSE* improves the CLIP-T while preserving the DINO; achieved with significantly fewer resources.

However, a significant gap remains between finetuning-based and fast P-T2I methods. We further perform concept-specific fine-tuning (as described in Section 3.3). As shown in Table 2, *λ-ECLIPSE* outperforms the DreamBooth and BLIP-Diffusion in terms of concept alignment (DINO)

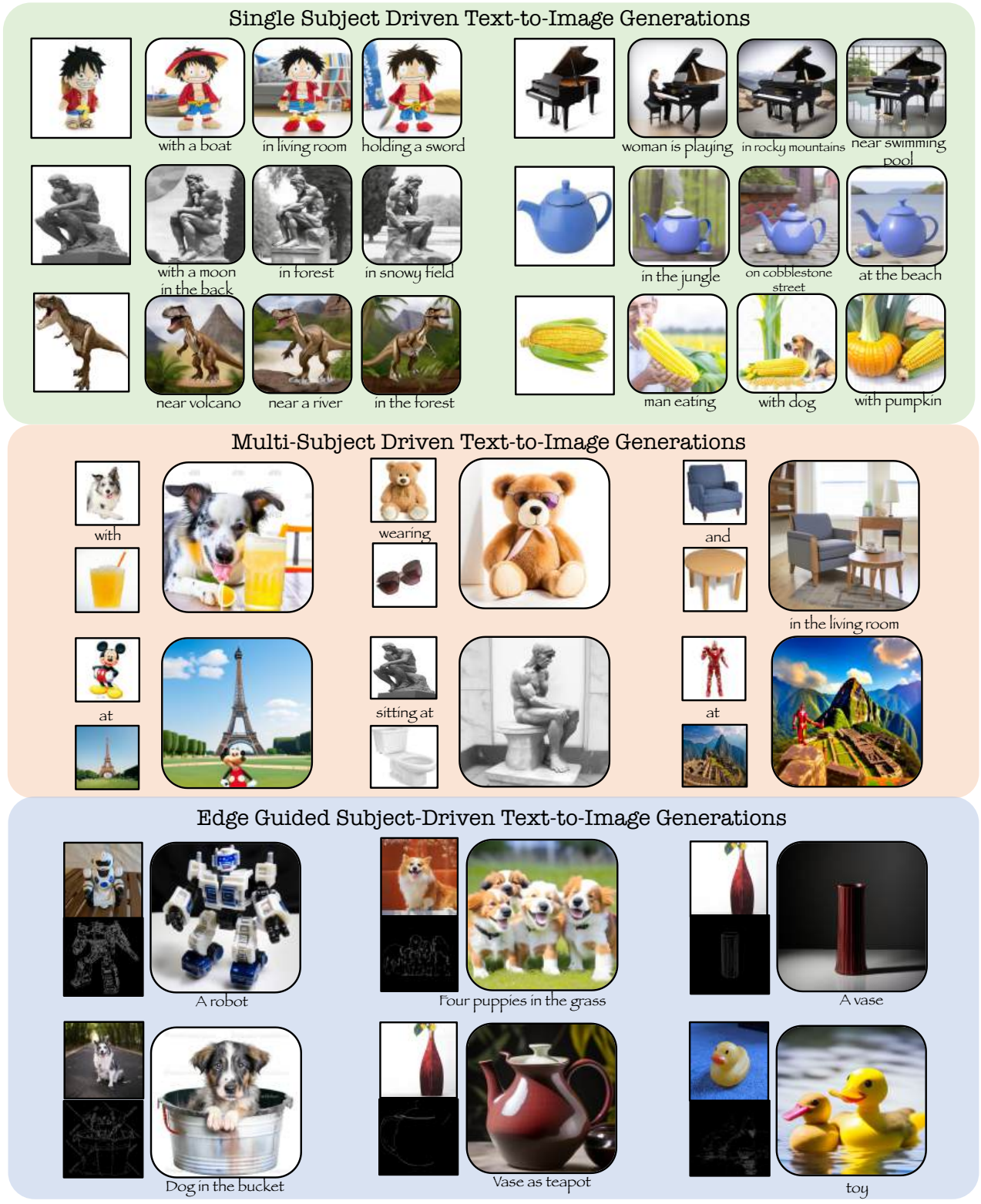

Figure 5: Qualitative results categorized by generative capabilities.

Table 4: **Quantitative comparisons of different methodologies on Multibench.** The **Bold** and underline represent the metric-specific first and second-ranked methods on each metric, respectively.

	Two Subjects			Three Subjects	
	Kosmos-G	**Emu2**	λ-*ECLIPSE*	**Emu2**	λ-*ECLIPSE*
DINO (↑)	**0.4549**	0.4451	0.4478	0.3168	**0.3420**
CLIP-I (↑)	**0.7759**	0.7397	0.7409	0.6231	**0.6463**
CLIP-T (↑)	0.2493	0.2673	**0.3327**	0.2819	**0.3469**

Table 5: **Quantitative results of Canny edge controlled P-T2I of different methodologies on Dreambench.** The **Bold** and underline represent the metric-specific first and second-ranked methods, respectively. Red highlighted numbers indicate the relative percentage drop for concept alignment compared to Table 2.

Method	**DINO** (↑)	**CLIP-I** (↑)	**CLIP-T** (↑)
BLIP-Diffusion*	0.4234$_{29.7\%}$	0.7119	0.3152
IP-Adapter*	0.4281$_{31.9\%}$	0.7315	0.3034
λ-*ECLIPSE**	**0.5173**$_{14.3\%}$	**0.7437**	**0.3158**

while maintaining the performance on composition alignment (CLIP-T). Notably, Multibench results (Table 4) indicate that λ-*ECLIPSE* significantly outperforms the Kosmos-G (2B params) and Emu2 (37B params) in terms of CLIP-T while maintaining the DINO performance. Therefore, we can conclude that λ-*ECLIPSE* is the most resource-efficient compared, especially when compared to the MLLM-based methods.

Qualitative comparisons. In Figure 4, we present a range of single subject-specific images generated by various methodologies including BLIP-Diffusion, IP-Adapter, Kosmos-G, Emu2, and λ-*ECLIPSE*. λ-*ECLIPSE* demonstrates exemplary proficiency in composition while ensuring concept alignment. In contrast, the baselines often overemphasize reference images or exhibit concept dilution, leading to higher concept alignment but compromised composition. Interestingly, we find that Emu2 can capture the single-subjects but it fails to reproduce them with complex text compositions (as shown in Figure 4). Similarly, Figure 6a exhibits λ-*ECLIPSE*'s multi-concept generation prowess, in comparison to ZipLoRA (fine-tuning-based approach) along with Kosmos-G and Emu2 (Multimodal LLM-based approaches), underscoring its capability to rival compute-intensive methods. We discuss additional examples and limitations in the appendix. That said, even though λ-*ECLIPSE* improves the performance over the baselines, this is still not enough and it signifies the challenges associated with fast multi-concept personalization.

Canny edge controlled image generation. As shown in Figure 6b, the baseline (BLIP-Diffusion) adheres strictly to the imposed edge maps, often at the cost of concept retention (rows 1, 3, and 4). This leads to a large number of unwanted artifacts in the generated images. To further ground this behavior, we first generated images using Stable Diffusion v1.5 for Dreambench prompts without customization then we extracted the Canny edge map and used this edge map to control the subject-driven image generations. At last, we report the performance in Table 5. It can be observed that both baselines IP-Adapter and BLIP-Diffusion drop the DINO score by 30%, which follows the qualitative results. While λ-*ECLIPSE* do not follow the Canny edge precisely but preserves the concept alignment and improves the performance relatively by 21%.

Ablations. We extend our study to evaluate the individual contributions of different components in λ-*ECLIPSE*. Initially, the model's performance with solely the projection loss (referenced in Eq.1) is assessed. Subsequent experiments involve training λ-*ECLIPSE* variants with varying hyperparameters for the contrastive loss, specifically λ values of 0.2 and 0.5. A comparative analysis of these baselines is conducted against the fully equipped λ-*ECLIPSE* model, which incorporates $\mathcal{L}_{prior}$ (Eq.1) with $\lambda = 0.2$ and utilizes Canny edge maps during training. Relying solely on projection loss results in high concept alignment but compromises compositions (Table 6). The contrastive loss variant with $\lambda = 0.5$ enhances composition alignment at the expense of concept alignment, whereas $\lambda = 0.2$ achieves a more balanced performance. Crucially, the integration of

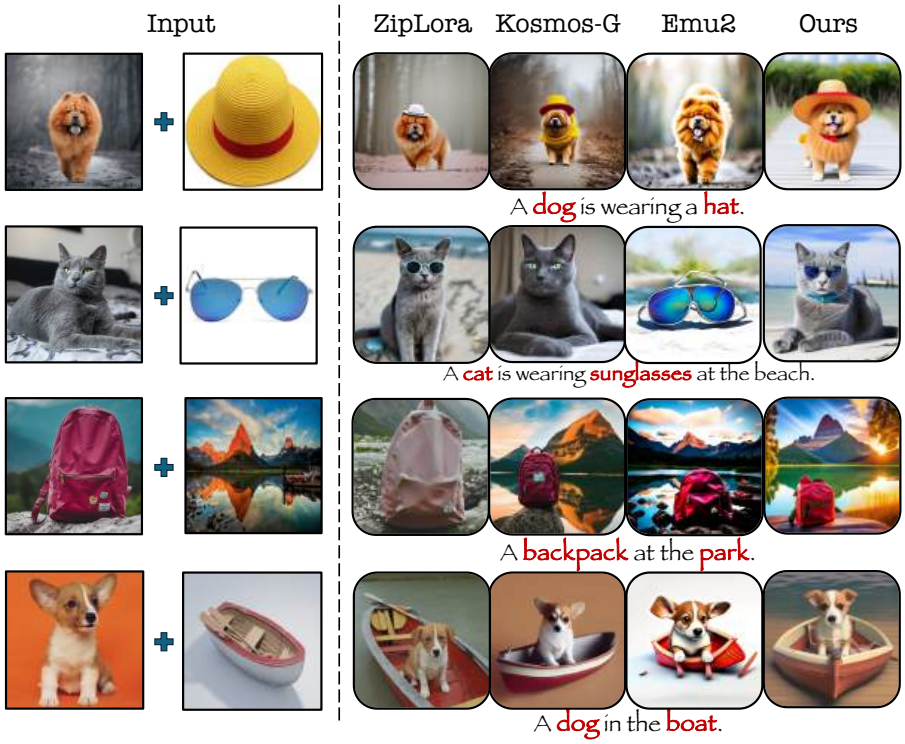

(a) **Multi-subject qualitative examples**.

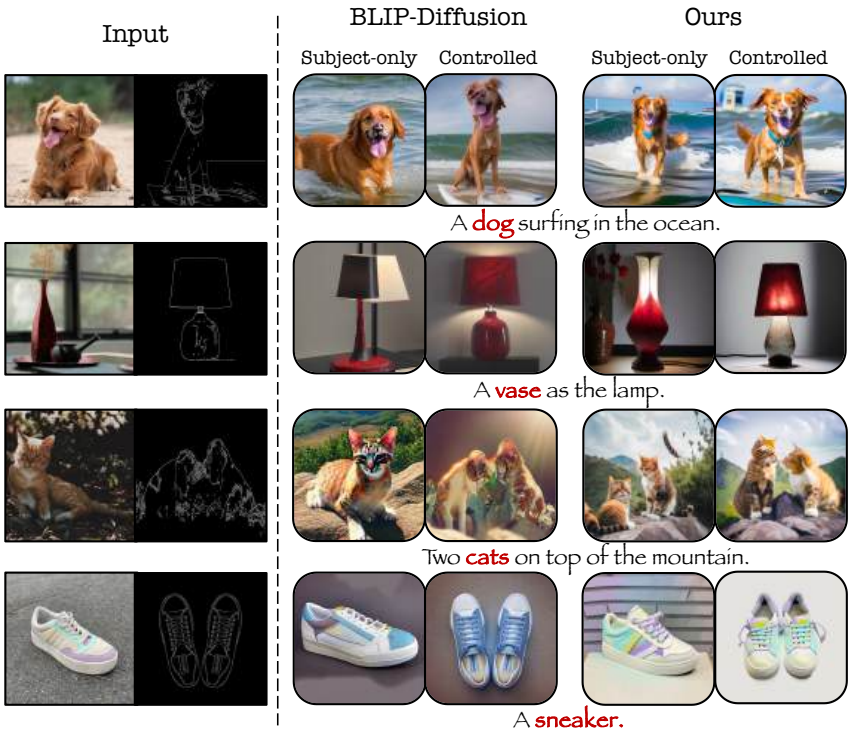

(b) **Qualitative examples for edge-guided P-T2I**.

Figure 6: **Qualitative comparison** between λ-*ECLIPSE* and other baselines.

Table 6: **Ablation studies** w.r.t. to the key components of λ-*ECLIPSE* design. We report the concept and composition alignment for single-subject T2I using CCD ($\downarrow$) on the ConceptBed benchmark.

Model	Concept Alignment ($\downarrow$)	Composition Alignment ($\downarrow$)
Projection loss (i.e. λ=0.0)	0.394	0.008
w/ contrastive loss (λ=0.5)	0.435	**-0.043**
w/ contrastive loss (λ=0.2)	0.402	-0.026
w/ edge conditions (λ=0.2)	**0.362**	-0.020

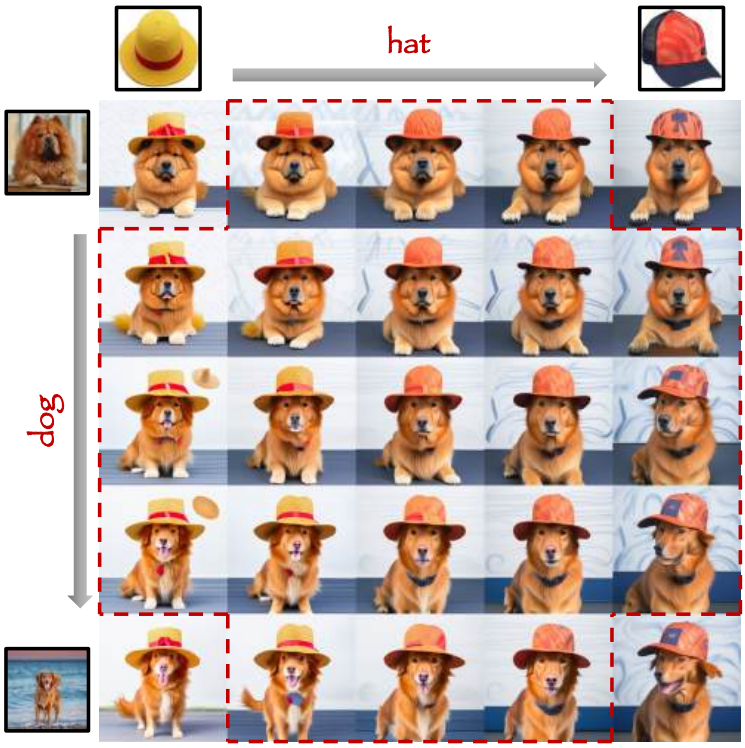

Figure 7: **Interpolation between four concepts.** Here, we estimate the image embedding using λ-*ECLIPSE* corresponding to each corner and then interpolate from top to bottom and left to right. At last, we use the Kandinsky v2.2 diffusion UNet model to generate the images with fixed random seeds from these sets of image embeddings.

Canny edge maps during training optimally balances both alignments and, specifically, improves the concept alignment. The negative values indicate that the CCD oracle model is highly confident in the generated images.

Multi-subject interpolation. A key attribute of the CLIP latent space is the ability to perform smooth interpolation between two sets of embeddings. We conducted experiments to demonstrate λ-*ECLIPSE*'s ability to learn and replicate this smooth latent space transition. We selected two distinct dog breeds (<dog1>, <dog2>) and two types of hats (<hat1>, <hat2>) as the concepts. λ-*ECLIPSE* was then used to estimate image embeddings for all four possible combinations, each corresponding to the input phrase "a <dog> wearing a <hat>." Fig. 7 showcases a gradual and seamless transition in the synthesized images from the top left to the bottom right. Unlike current diffusion models, which often exhibit sensitivity to input variations requiring numerous iterations of user interactions for desired outcomes, λ-*ECLIPSE* inherits CLIP's smooth latent space. This not only facilitates progressive changes in the conceptual domain but also extends the model's utility by enabling personalized **multi-subject interpolations**.

5 Conclusion

In this paper, we have introduced a novel diffusion-free methodology for personalized text-to-image (P-T2I) applications, utilizing the latent space of the pre-trained CLIP model with high efficiency. Our λ-*ECLIPSE* model, trained on an image-text interleaved dataset, achieves the capability to execute single-concept, multi-concept, and edge-guided controlled P-T2I tasks using a singular model framework, while simultaneously minimizing resource utilization. Notably, λ-*ECLIPSE* sets a new benchmark in achieving competitive performance in terms of concept and composition alignment. Furthermore, our research illuminates the potential of λ-*ECLIPSE* in exploring and leveraging the smooth latent space. This capability unlocks new avenues for interpolating between multiple concepts and their amalgamation, thereby generating entirely novel concepts. Our findings underscore a promising pathway to improve MLLMs to effectively control the pre-trained diffusion image models without necessitating extra supervision.

Acknowledgments

This work was supported by NSF RI grants #1750082, #2132724, and CPS grant #2038666. We thank the Research Computing (RC) at Arizona State University (ASU) for providing computing resources. The views and opinions of the authors expressed herein do not necessarily state or reflect those of the funding agencies and employers.

References

[1] Yuval Alaluf, Elad Richardson, Gal Metzer, and Daniel Cohen-Or. A neural space-time representation for text-to-image personalization. *ACM Transactions on Graphics (TOG)*, 42(6):1–10, 2023. 20

[2] Jean-Baptiste Alayrac, Jeff Donahue, Pauline Luc, Antoine Miech, Iain Barr, Yana Hasson, Karel Lenc, Arthur Mensch, Katherine Millican, Malcolm Reynolds, et al. Flamingo: a visual language model for few-shot learning. *Advances in Neural Information Processing Systems*, 35:23716–23736, 2022. 6

[3] Moab Arar, Rinon Gal, Yuval Atzmon, Gal Chechik, Daniel Cohen-Or, Ariel Shamir, and Amit H. Bermano. Domain-agnostic tuning-encoder for fast personalization of text-to-image models. In *SIGGRAPH Asia 2023 Conference Papers*, pages 1–10, 2023. 20

[4] Omri Avrahami, Kfir Aberman, Ohad Fried, Daniel Cohen-Or, and Dani Lischinski. Break-a-scene: Extracting multiple concepts from a single image. *arXiv preprint arXiv:2305.16311*, 2023. 4, 20

[5] James Betker, Gabriel Goh, Li Jing, Tim Brooks, Jianfeng Wang, Linjie Li, Long Ouyang, Juntang Zhuang, Joyce Lee, Yufei Guo, et al. Improving image generation with better captions. *Computer Science. https://cdn. openai. com/papers/dall-e-3. pdf*, 2:3, 2023. 3

[6] Hong Chen, Yipeng Zhang, Xin Wang, Xuguang Duan, Yuwei Zhou, and Wenwu Zhu. Disenbooth: Disentangled parameter-efficient tuning for subject-driven text-to-image generation. *arXiv preprint arXiv:2305.03374*, 2023. 20

[7] Junsong Chen, Jincheng Yu, Chongjian Ge, Lewei Yao, Enze Xie, Yue Wu, Zhongdao Wang, James Kwok, Ping Luo, Huchuan Lu, et al. Pixart-alpha: Fast training of diffusion transformer for photorealistic text-to-image synthesis. *arXiv preprint arXiv:2310.00426*, 2023. 3

[8] Wenhu Chen, Hexiang Hu, Yandong Li, Nataniel Rui, Xuhui Jia, Ming-Wei Chang, and William W Cohen. Subject-driven text-to-image generation via apprenticeship learning. *arXiv preprint arXiv:2304.00186*, 2023. 20

[9] Wenhu Chen, Hexiang Hu, Chitwan Saharia, and William W Cohen. Re-imagen: Retrieval-augmented text-to-image generator. In *The Eleventh International Conference on Learning Representations*, 2022. 20

[10] Ming Ding, Zhuoyi Yang, Wenyi Hong, Wendi Zheng, Chang Zhou, Da Yin, Junyang Lin, Xu Zou, Zhou Shao, Hongxia Yang, et al. Cogview: Mastering text-to-image generation via transformers. *Advances in Neural Information Processing Systems*, 34:19822–19835, 2021. 3

[11] Rinon Gal, Yuval Alaluf, Yuval Atzmon, Or Patashnik, Amit Haim Bermano, Gal Chechik, and Daniel Cohen-or. An image is worth one word: Personalizing text-to-image generation using textual inversion. In *The Eleventh International Conference on Learning Representations*, 2022. 2, 3, 20

[12] Rinon Gal, Moab Arar, Yuval Atzmon, Amit H Bermano, Gal Chechik, and Daniel Cohen-Or. Encoder-based domain tuning for fast personalization of text-to-image models. *ACM Transactions on Graphics (TOG)*, 42(4):1–13, 2023. 2, 20

[13] Yuying Ge, Sijie Zhao, Ziyun Zeng, Yixiao Ge, Chen Li, Xintao Wang, and Ying Shan. Making llama see and draw with seed tokenizer. *arXiv preprint arXiv:2310.01218*, 2023. 2

[14] Yuchao Gu, Xintao Wang, Jay Zhangjie Wu, Yujun Shi, Yunpeng Chen, Zihan Fan, Wuyou Xiao, Rui Zhao, Shuning Chang, Weijia Wu, et al. Mix-of-show: Decentralized low-rank adaptation for multi-concept customization of diffusion models. *arXiv preprint arXiv:2305.18292*, 2023. 4, 20

[15] Ligong Han, Yinxiao Li, Han Zhang, Peyman Milanfar, Dimitris Metaxas, and Feng Yang. Svdiff: Compact parameter space for diffusion fine-tuning. *arXiv preprint arXiv:2303.11305*, 2023. 20

[16] Edward J Hu, Phillip Wallis, Zeyuan Allen-Zhu, Yuanzhi Li, Shean Wang, Lu Wang, Weizhu Chen, et al. Lora: Low-rank adaptation of large language models. In *International Conference on Learning Representations*, 2021. 3

[17] Xuhui Jia, Yang Zhao, Kelvin CK Chan, Yandong Li, Han Zhang, Boqing Gong, Tingbo Hou, Huisheng Wang, and Yu-Chuan Su. Taming encoder for zero fine-tuning image customization with text-to-image diffusion models. *arXiv preprint arXiv:2304.02642*, 2023. 20

[18] Changhoon Kim, Kyle Min, Maitreya Patel, Sheng Cheng, and Yezhou Yang. Wouaf: Weight modulation for user attribution and fingerprinting in text-to-image diffusion models. *arXiv preprint arXiv:2306.04744*, 2023. 22

[19] Alexander Kirillov, Eric Mintun, Nikhila Ravi, Hanzi Mao, Chloe Rolland, Laura Gustafson, Tete Xiao, Spencer Whitehead, Alexander C Berg, Wan-Yen Lo, et al. Segment anything. *arXiv preprint arXiv:2304.02643*, 2023. 7, 17

[20] Nupur Kumari, Bingliang Zhang, Richard Zhang, Eli Shechtman, and Jun-Yan Zhu. Multi-concept customization of text-to-image diffusion. In *Proceedings of the IEEE/CVF Conference on Computer Vision and Pattern Recognition*, pages 1931–1941, 2023. 2, 3, 20

[21] Donghoon Lee, Jiseob Kim, Jisu Choi, Jongmin Kim, Minwoo Byeon, Woonhyuk Baek, and Saehoon Kim. Karlo-v1.0.alpha on coyo-100m and cc15m. https://github.com/kakaobrain/karlo, 2022. 3

[22] Dongxu Li, Junnan Li, and Steven CH Hoi. Blip-diffusion: Pre-trained subject representation for controllable text-to-image generation and editing. *arXiv preprint arXiv:2305.14720*, 2023. 3, 20

[23] Junnan Li, Dongxu Li, Silvio Savarese, and Steven Hoi. Blip-2: Bootstrapping language-image pre-training with frozen image encoders and large language models. *arXiv preprint arXiv:2301.12597*, 2023. 3

[24] Yuheng Li, Haotian Liu, Qingyang Wu, Fangzhou Mu, Jianwei Yang, Jianfeng Gao, Chunyuan Li, and Yong Jae Lee. Gligen: Open-set grounded text-to-image generation. In *Proceedings of the IEEE/CVF Conference on Computer Vision and Pattern Recognition*, pages 22511–22521, 2023. 4

[25] Shilong Liu, Zhaoyang Zeng, Tianhe Ren, Feng Li, Hao Zhang, Jie Yang, Chunyuan Li, Jianwei Yang, Hang Su, Jun Zhu, et al. Grounding dino: Marrying dino with grounded pre-training for open-set object detection. *arXiv preprint arXiv:2303.05499*, 2023. 7, 17

[26] Zhiheng Liu, Ruili Feng, Kai Zhu, Yifei Zhang, Kecheng Zheng, Yu Liu, Deli Zhao, Jingren Zhou, and Yang Cao. Cones: Concept neurons in diffusion models for customized generation. *arXiv preprint arXiv:2303.05125*, 2023. 20

[27] Zhiheng Liu, Yifei Zhang, Yujun Shen, Kecheng Zheng, Kai Zhu, Ruili Feng, Yu Liu, Deli Zhao, Jingren Zhou, and Yang Cao. Customizable image synthesis with multiple subjects. In *Thirty-seventh Conference on Neural Information Processing Systems*, 2023. 20

[28] Jian Ma, Junhao Liang, Chen Chen, and Haonan Lu. Subject-diffusion: Open domain personalized text-to-image generation without test-time fine-tuning. *arXiv preprint arXiv:2307.11410*, 2023. 3, 4, 17, 20

[29] Yiyang Ma, Huan Yang, Wenjing Wang, Jianlong Fu, and Jiaying Liu. Unified multi-modal latent diffusion for joint subject and text conditional image generation. *arXiv preprint arXiv:2303.09319*, 2023. 20

[30] Xichen Pan, Li Dong, Shaohan Huang, Zhiliang Peng, Wenhu Chen, and Furu Wei. Kosmos-g: Generating images in context with multimodal large language models. *arXiv preprint arXiv:2310.02992*, 2023. 2, 3, 20

[31] Maitreya Patel, Tejas Gokhale, Chitta Baral, and Yezhou Yang. Conceptbed: Evaluating concept learning abilities of text-to-image diffusion models. *arXiv preprint arXiv:2306.04695*, 2023. 7, 8

[32] Maitreya Patel, Changhoon Kim, Sheng Cheng, Chitta Baral, and Yezhou Yang. Eclipse: A resource-efficient text-to-image prior for image generations. *arXiv preprint arXiv:2312.04655*, 2023. 2, 5

[33] Can Qin, Shu Zhang, Ning Yu, Yihao Feng, Xinyi Yang, Yingbo Zhou, Huan Wang, Juan Carlos Niebles, Caiming Xiong, Silvio Savarese, et al. Unicontrol: A unified diffusion model for controllable visual generation in the wild. *arXiv preprint arXiv:2305.11147*, 2023. 4

[34] Alec Radford, Jong Wook Kim, Chris Hallacy, Aditya Ramesh, Gabriel Goh, Sandhini Agarwal, Girish Sastry, Amanda Askell, Pamela Mishkin, Jack Clark, et al. Learning transferable visual models from natural language supervision. In *International conference on machine learning*, pages 8748–8763. PMLR, 2021. 3

[35] Aditya Ramesh, Prafulla Dhariwal, Alex Nichol, Casey Chu, and Mark Chen. Hierarchical text-conditional image generation with clip latents. *arXiv preprint arXiv:2204.06125*, 1(2):3, 2022. 2, 3

[36] Aditya Ramesh, Mikhail Pavlov, Gabriel Goh, Scott Gray, Chelsea Voss, Alec Radford, Mark Chen, and Ilya Sutskever. Zero-shot text-to-image generation. In *International Conference on Machine Learning*, pages 8821–8831. PMLR, 2021. 3

[37] Anton Razzhigaev, Arseniy Shakhmatov, Anastasia Maltseva, Vladimir Arkhipkin, Igor Pavlov, Ilya Ryabov, Angelina Kuts, Alexander Panchenko, Andrey Kuznetsov, and Denis Dimitrov. Kandinsky: An improved text-to-image synthesis with image prior and latent diffusion. In *Proceedings of the 2023 Conference on Empirical Methods in Natural Language Processing: System Demonstrations*, pages 286–295, 2023. 2, 3

[38] Robin Rombach, Andreas Blattmann, Dominik Lorenz, Patrick Esser, and Björn Ommer. High-resolution image synthesis with latent diffusion models. In *Proceedings of the IEEE/CVF conference on computer vision and pattern recognition*, pages 10684–10695, 2022. 2, 3, 17

[39] Nataniel Ruiz, Yuanzhen Li, Varun Jampani, Yael Pritch, Michael Rubinstein, and Kfir Aberman. Dreambooth: Fine tuning text-to-image diffusion models for subject-driven generation. In *Proceedings of the IEEE/CVF Conference on Computer Vision and Pattern Recognition*, pages 22500–22510, 2023. 2, 3, 5, 7, 20

[40] Nataniel Ruiz, Yuanzhen Li, Varun Jampani, Wei Wei, Tingbo Hou, Yael Pritch, Neal Wadhwa, Michael Rubinstein, and Kfir Aberman. Hyperdreambooth: Hypernetworks for fast personalization of text-to-image models. *arXiv preprint arXiv:2307.06949*, 2023. 2, 20

[41] Chitwan Saharia, William Chan, Saurabh Saxena, Lala Li, Jay Whang, Emily L Denton, Kamyar Ghasemipour, Raphael Gontijo Lopes, Burcu Karagol Ayan, Tim Salimans, et al. Photorealistic text-to-image diffusion models with deep language understanding. *Advances in Neural Information Processing Systems*, 35:36479–36494, 2022. 3

[42] Christoph Schuhmann, Romain Beaumont, Richard Vencu, Cade Gordon, Ross Wightman, Mehdi Cherti, Theo Coombes, Aarush Katta, Clayton Mullis, Mitchell Wortsman, et al. Laion-5b: An open large-scale dataset for training next generation image-text models. *Advances in Neural Information Processing Systems*, 35:25278–25294, 2022. 7

[43] Viraj Shah, Nataniel Ruiz, Forrester Cole, Erika Lu, Svetlana Lazebnik, Yuanzhen Li, and Varun Jampani. Ziplora: Any subject in any style by effectively merging loras. *arXiv preprint arXiv:2311.13600*, 2023. 2, 4, 20

[44] Jing Shi, Wei Xiong, Zhe Lin, and Hyun Joon Jung. Instantbooth: Personalized text-to-image generation without test-time finetuning. *arXiv preprint arXiv:2304.03411*, 2023. 20

[45] James Seale Smith, Yen-Chang Hsu, Lingyu Zhang, Ting Hua, Zsolt Kira, Yilin Shen, and Hongxia Jin. Continual diffusion: Continual customization of text-to-image diffusion with c-lora. *arXiv preprint arXiv:2304.06027*, 2023. 20

[46] Quan Sun, Yufeng Cui, Xiaosong Zhang, Fan Zhang, Qiying Yu, Zhengxiong Luo, Yueze Wang, Yongming Rao, Jingjing Liu, Tiejun Huang, et al. Generative multimodal models are in-context learners. *arXiv preprint arXiv:2312.13286*, 2023. 2, 3, 4, 20

[47] Yoad Tewel, Rinon Gal, Gal Chechik, and Yuval Atzmon. Key-locked rank one editing for text-to-image personalization. In *ACM SIGGRAPH 2023 Conference Proceedings*, pages 1–11, 2023. 2, 3, 20

[48] Narek Tumanyan, Michal Geyer, Shai Bagon, and Tali Dekel. Plug-and-play diffusion features for text-driven image-to-image translation. In *Proceedings of the IEEE/CVF Conference on Computer Vision and Pattern Recognition*, pages 1921–1930, 2023. 2, 20

[49] Andrey Voynov, Qinghao Chu, Daniel Cohen-Or, and Kfir Aberman. $p+$: Extended textual conditioning in text-to-image generation. *arXiv preprint arXiv:2303.09522*, 2023. 20

[50] Yuxiang Wei, Yabo Zhang, Zhilong Ji, Jinfeng Bai, Lei Zhang, and Wangmeng Zuo. Elite: Encoding visual concepts into textual embeddings for customized text-to-image generation. *2023 IEEE/CVF International Conference on Computer Vision (ICCV)*, pages 15897–15907, 2023. 2, 3, 20

[51] Guangxuan Xiao, Tianwei Yin, William T Freeman, Frédo Durand, and Song Han. Fastcomposer: Tuning-free multi-subject image generation with localized attention. *arXiv preprint arXiv:2305.10431*, 2023. 20

[52] Hu Ye, Jun Zhang, Sibo Liu, Xiao Han, and Wei Yang. Ip-adapter: Text compatible image prompt adapter for text-to-image diffusion models. *arXiv preprint arXiv:2308.06721*, 2023. 2, 3, 20

[53] Lvmin Zhang, Anyi Rao, and Maneesh Agrawala. Adding conditional control to text-to-image diffusion models. In *Proceedings of the IEEE/CVF International Conference on Computer Vision*, pages 3836–3847, 2023. 4

[54] Yuxuan Zhang, Jiaming Liu, Yiren Song, Rui Wang, Hao Tang, Jinpeng Yu, Huaxia Li, Xu Tang, Yao Hu, Han Pan, et al. Ssr-encoder: Encoding selective subject representation for subject-driven generation. *arXiv preprint arXiv:2312.16272*, 2023. 20

[55] Ruoyu Zhao, Mingrui Zhu, Shiyin Dong, Nannan Wang, and Xinbo Gao. Catversion: Concatenating embeddings for diffusion-based text-to-image personalization. *arXiv preprint arXiv:2311.14631*, 2023. 20

A Preliminaries for T2I Diffusion Models

As evidenced in numerous contemporary studies regarding T2I models, Stable Diffusion (SD) [38] has emerged as a predominant backbone for T2I models. SD involves training diffusion models in latent space, reversing a forward diffusion process that introduces noise into the image. A notable feature of SD is its integration of cross-attention, facilitating various conditions like text input. Operating in VQ-VAE latent space, SD not only achieves exceptional generative performance surpassing that in pixel space but also significantly reduces the computational demands.

UnCLIP models (such as DALL-E 2) are very similar to the Stable Diffusion. In contrast, the UnCLIP takes the modular approach. UnCLIP first trains the diffusion text-to-image to the image prior (f_θ) to estimate the image embeddings (z_x) from the text embeddings (z_y). In parallel, a UNet-like diffusion image generator (h_ϕ) is trained to generate images (x) conditioned on ground truth vision embeddings (z_x).

Traditionally, T2I prior is modeled to estimate x_0-prediction instead of ϵ-prediction. Given the forward function $z_x^{(t)} \sim q(t, z_x)$, the goal of f_θ is to directly estimate z_x for all timesteps $t \sim [0, T]$ as:

$$\mathcal{L}_{prior} = \mathop{\mathbb{E}}_{\substack{t\sim[0,T],\\ z_x^{(t)}\sim q(t,z_x)}} \Big[||z_x - f_\theta(z_x^{(t)}, t, z_y)||_2^2\Big]. \tag{3}$$

ECLIPSE proposes the contrastive learning strategy (Eq. 1 – main paper) instead of minimizing Eq. 3. The diffusion image generator is trained by following standard ϵ-prediction formulation. Here, h_ϕ will estimate the ground truth added Gaussian noise $\epsilon \sim N(0, I)$, given the noise image $X^{(t)}$ for all timesteps $t \sim [0, T]$ and input conditions (such as z_x, z_y).

$$\mathcal{L}_{decoder} = \mathop{\mathbb{E}}_{\substack{\epsilon\sim N(0,I)\\ t\sim[0,T],\\ (z_x,\ z_y)}} \Big[||\epsilon - h_\phi(x^{(t)}, t, z_x, z_y)||_2^2\Big]. \tag{4}$$

For models like Kandinsky v2.2, we drop the z_y to condition the model on z_x. Therefore, λ-*ECLIPSE* also only conditions the image generation with z_y in the prior stage.

B Image-Text Interleaved Training Details

Dataset Creation In constructing the dataset, we adhered to the data processing pipeline of Subject Diffusion [28]. We utilized the LAION-5B High-Res dataset, requiring a minimum image size of 1024x1024 resolution. Original captions were replaced with new captions generated by BLIP-2 (flan-t5-xl)[3]. Subjects were extracted using Spacy[4]. For each subject, we identified bounding boxes employing Grounding DINO [25], setting both box-threshold and text-threshold values to 0.2. We retained images with 1 to 8 detected bounding boxes, discarding the rest. Additionally, captions with multiple instances of identical objects were filtered, allowing a maximum of 6 identical objects. Following bounding box detection, individual subject masks were isolated using Segment-Anything (SAM) [19]. To enhance the efficiency of the training process, we pre-processed the dataset by pre-extracting features from CLIP vision and text encoders. During this phase, images predominantly featuring a background (white portion) exceeding 10% of the total area were excluded. We preserved bounding boxes with a width-height ratio ranging from 0.08 to 0.7 and logit scores of at least 0.3. Masks constituting less than 40% of the bounding box area were discarded. For the selection of subjects in images, we constrained the range to 1-4 subjects per image, excluding those with more than 4 subjects. At last, the interleaved image-text examples with respective ground truth images are shown in Figure 8.

Dataset Statistics In the final analysis, our dataset comprised a total of 1,990,123 images. The distribution of subjects per image exhibited a range from 1 to 4, with the following breakdown: 1,479,785 images featuring one subject, 432,831 images with two subjects, 65,597 images containing

[3] https://huggingface.co/Salesforce/blip2-flan-t5-xl
[4] https://spacy.io

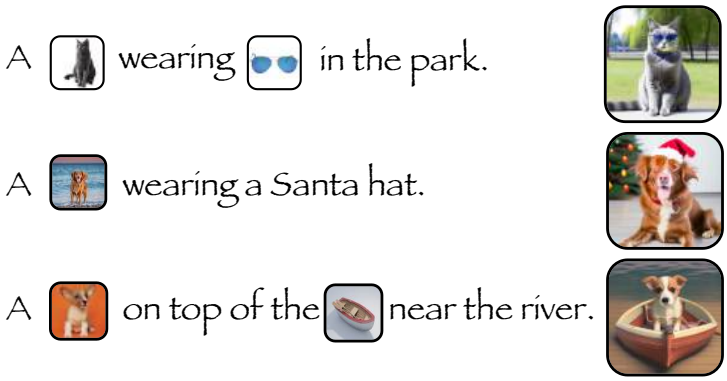

Figure 8: **Examples of image-text interleaved training data.** The left column shows the input of the prior model and the right images shows the ground truth corresponding images. Note: these examples are generated from λ-*ECLIPSE* for better interpretability.

three subjects, and 11,910 images showcasing four subjects. The overall count of unique subjects acquired from this dataset amounted to 30,358. We partitioned our dataset into an 80:20 split between training and validation, reserving the remaining 1.6 million images for training and the rest for validation.

C Implementation Details

The λ-*ECLIPSE* transformer prior architecture is significantly more compact compared to other Text-to-Image (T2I) methodologies. Our model employs a configuration of 16 Attention Heads, each with a dimension size of 32, alongside a total of 10 layers. Additionally, the embedding dimension size for our model is set at 1280, supplemented by 4 auxiliary embeddings (including, one for canny edge map). As λ-*ECLIPSE* is not a diffusion prior model, we do not keep time embedding layers. Overall, the λ-*ECLIPSE* model comprises approximately 34 million parameters, establishing it as a streamlined yet effective solution for Personalaized-T2I. Notably, the standard UnCLIP T2I priors contain 1 billion parameters.

D λ-*ECLIPSE* with Finetuning

As demonstrated in the main paper (Table 2), the superiority of fine-tuning-based personalization methodologies, whether applied to single-subject or multi-subject frameworks, over non-fine-tuning alternatives is evident. Consequently, we have expanded our analysis through additional fine-tuning of the λ-*ECLIPSE*.

Experimental Setup. Given that λ-*ECLIPSE* effectively trains the T2I prior, capturing concept-specific features to a significant degree, we opted not to further optimize this component. Our focus shifted to exclusively fine-tuning the diffusion UNet model (h_ϕ), employing the AdamW optimizer at a learning rate of 1e-5, without warm-up steps. For the DreamBooth application within the Stable Diffusion v1.5 model, we selected a learning rate of 5e-6, maintaining consistency in other hyperparameters. To simplify, we excluded the use of a prior preservation regularizer and conducted training on the Dreambench platform using a single RTX A6000 GPU.

Results. Our findings, illustrated in Figure 9, reveal that λ-*ECLIPSE* and DreamBooth exhibit improved performance with incremental fine-tuning steps. Notably, the DINO score improved from 0.61 to 0.68 with few optimization steps and outperforms the baselines (see Table 2). A detailed analysis indicates that while DreamBooth's DINO score improves, its CLIP-T performance diminishes, hinting at concept overfitting. Conversely, λ-*ECLIPSE* consistently improves in DINO scoring without adversely impacting the CLIP-T performance, underscoring the efficacy of our image-text interleaved training approach at the prior stage. Qualitative comparisons, as shown in Figure 10, further highlight the benefits of fine-tuning λ-*ECLIPSE* with minimal steps.

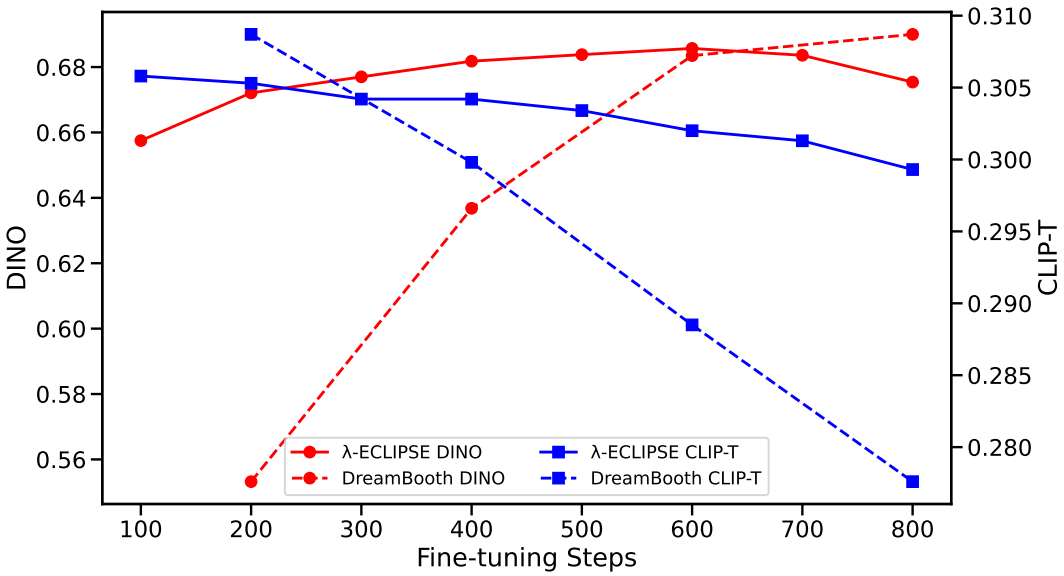

Figure 9: **DreamBooth (Stable Diffusion v1.5)** ***vs.*** λ*-ECLIPSE* **(with fine-tuning)** *w.r.t.* DINO and CLIP-T metrics on Dreambench.

Advantages of fine-tuning λ*-ECLIPSE.* The fine-tuning of λ*-ECLIPSE*, in comparison to the baselines, reveals two key benefits: 1) Achieving state-of-the-art (SOTA) performance within a few finetuning steps. 2) Unlike the Stable Diffusion model, which exhibits catastrophic forgetting of nearby concepts post-DreamBooth fine-tuning, λ*-ECLIPSE* maintains previous knowledge. This suggests that a single model is sufficient to effectively fine-tune across multiple concepts together.

This analysis underscores the strategic advantages and enhanced efficiency of fine-tuning λ*-ECLIPSE* for personalized applications in complex visual data processing.

E Extended P-T2I Baselines Comparison

We further expand our comparative analysis of P-T2I methods encompassing a total of 33 approaches including ours and parallel works. Table 7 summarizes them into four crucial aspects: 1) multi-subject support, 2) fine-tuning free, 3) base model types, and 4) the required number of input images. To summarize, λ*-ECLIPSE* is the only methodology built on top of the UnCLIP models while supporting multi-subject driven image generation with fine-tuning free, and only requires a single reference image input for the training. We detail the comparison below:

Multi-Subject Generation. Multi-subject generation enables users to integrate multiple personal subjects to generate an image that follows the text prompts and aligns with all the concept visuals. In total, 15 of the 33 methods offer this capability, while 6 methods support fast multi-subject personalization, others demand separate training for each subject to be learned and then an additional fusing step for combining the learned subjects is required (i.e. Zip-LoRA, Mix-of-Show). Among these methods, only a few can learn auxiliary guided information such as canny edge, depth maps, or open-pose and adapt style variation (i.e. Kosmos-G).

Fine-tuning Free (Fast Personalization). Many methods require test-time fine-tuning. Each varies on which part alteration occurs, as early models tend to modify the whole UNet. In contrast, recent models tune a small portion of the cross-attention layers or introduce additional layers performing as adapters. In our analysis of P-T2I methodologies, 14 out of 33 methods employ a finetuning-free approach which enables fast personalization.

Diffusion Independent. A majority of the reviewed models utilize diffusion models, with Stable Diffusion being the predominant choice, spanning versions 1.4, 1.5, 2.1, and XL. Few adapt Imagen (SuTi, Taming) and Mix-of-show employs ChillOutMix as their pre-trained model, known for its

Table 7: **The detailed overview of subject-driven text-to-image generative methodologies.** * represents the backbone base models listed are subject to potential updates or modifications.

Method	Multi-Subject	Finetuning-Free	Base-Model	# of Input Images
Re-Imagen [9]	✗	✓	Imagen	Single
Textual Inversion [11]	✗	✗	SDv1.4	Multiple
DreamBooth [39]	✗	✗	SDv1.4	Multiple
Custom Diffusion [20]	✓	✗	SDv1.4	Multiple
ELITE [50]	✗	✓	SDv1.4	Single
E4T [12]	✗	✗	SD	Single
Cones [26]	✓	✗	SDv1.4	Single
SVDiff [15]	✓	✗	SD	Multiple
UMM-Diffusion [29]	✗	✓	SDv1.5	Single
XTI [49]	✗	✗	SDv1.4	Multiple
Continual Diffusion [45]	✓	✗	-	Multiple
InstantBooth [44]	✗	✓	SDv1.4	Multiple
SuTi [8]	✗	✓	Imagen	Multiple
Taming [17]	✗	✓	Imagen	Single
BLIP-Diffusion [22]	✗	✓	SDv1.5	Single
Cones 2 [27]	✓	✗	SDv2.1	Single
DisenBooth [6]	✗	✗	SDv2.1	Single
FastComposer [51]	✓	✓	SDv1.5	Single
Perfusion [47]	✓	✗	SDv1.5	Multiple
Mix-of-Show [14]	✓	✗	Chilloutmix	Multiple
NeTI [1]	✗	✗	SDv1.4	Mulitple
Break-A-Scene [4]	✓	✗	SDv2.1	Single*
ViCo [48]	✗	✗	SDv1.4	Mulitple
Domain-Agnostic [3]	✗	✗	-	Single
Subject-Diffusion [28]	✓	✓	SDv2	Single
HyperDreamBooth [40]	✗	✗	SDv1.5	Single
IP-Adapter [52]	✗	✓	SDv1.5	Single
Kosmos-G [30]	✓	✓	SDv1.5	Single
Zip-LoRA [43]	✓	✗	SDXL	Multiple
CatVersion [55]	✗	✗	SDv1.5	Multiple
SSR-Encoder [54]	✓	✓	SDv1.5	Single
Emu2 [46]	✓	✓	SDXL	Single
λ-*ECLIPSE* **(ours)**	✓	✓	Kv2.2	Single

adeptness at preserving realistic concepts like human faces. A unique outlier in this landscape is our λ-*ECLIPSE*, the only one that eschews the use of any diffusion prior model.

Easiness of Use. A more user-friendly model typically requires a single reference image per subject, as opposed to multiple images of the same subject. In our study, 19 methods offer P-T2I capabilities with just one input image. In contrast, others often require 4 to 5 images of the subject. Additionally, some methods necessitate storage space for learned concepts, ranging from a few hundred kilobytes (e.g., Perfusion, HyperDreamBooth) to several megabytes (e.g., Zip-LoRA). Our method stands out by eliminating the need for individual concept pre-learning or storing any artifacts for P-T2I utilization, offering a streamlined, efficient user experience.

F Multibench Dataset

We provide additional qualitative results in Figure 5. For the multi-subject image benchmark, our dataset comprises 2,308 unique prompts, segmented into 904 two-subject and 1,476 three-subject prompts. This dataset integrates subjects from the original DreamBench dataset, featuring 30 distinct concepts. We expanded the dataset by incorporating additional concepts vital for two and three subject-specific prompts, such as various parks, hats, glasses, and more. Prompt templates and the count of unique subject categories featured in prompts are detailed in Tables 8 and 9, respectively. Overall, the dataset includes 217 two-subject compositions and 405 three-subject compositions, enriching the benchmark's diversity and comprehensiveness.

Table 8: **Example of prompt templates used for Multibench dataset.** Subjects presented in Table 9 are placed in {}.

Two subjects	Three subjects
{} in the {}	{} with a {} and {}
{} wearing a {}	{} is playing with {} in {}
{} chasing a {}	{} with {} in front of {}
{} looking at a {}	{} with a {} and a view of the {}
{} is sitting on a {}	{} with a {} and {} in the background
{} standing on a {}	
{} and {} playing in the garden	
{} and {} on top of the mountain	
{} and {} in the jungle	
{} and {} in the snow	
{} and {} on the beach	
{} and {} on a cobblestone street	
{} and {} standing next to each other	

Table 9: **Number of occurrences of unique subject categories.** The left side of the table are subjects used for two subjects prompts, and the right side of the table are subjects used for three subjects prompts.

Two subjects				Three subjects			
dog	76	boat	5	dog	81	rainbow	35
cat	76	park	4	stuffed animal	105	ruins	35
bird	76	ruins	9	toy	105	tower	35
horse	73	castle	5	cat	81	horse	81
guinea pig	73	desert	4	desert	60	bird	81
glasses	5	rainbow	5	hill	60	guinea pig	81
hat	5	candle	5	castle	45	guitar	25
tower	10	backpack	3	backpack	65	french horn	25
				can	130	vase	25
				candle	65	robot	25
				church	35		

G Qualitative Results & Failure Cases

In this section, we showcase a collection of detailed qualitative examples from the P-T2I generation process, highlighting the challenges of crafting complex compositions within λ-*ECLIPSE* and comparative models. As depicted in Figure 11, the complexity of the showcased examples progressively increases, illustrating a noticeable escalation in the intricacy of visual concepts from the top to the bottom of the figure. With the rising complexity, we note a universal decline in the ability of all methodologies, including λ-*ECLIPSE*, to preserve subject fidelity accurately. Interestingly, despite these challenges, λ-*ECLIPSE* demonstrates a better grasp of compositional integrity, unlike the baseline models which falter across all complexity levels.

Moreover, we present instances demonstrating the variability in outcomes produced by P-T2I methods across different trials. As illustrated in Figure 12, while there is a semblance of consistency in generating single and multiple concepts between models, Kosmos-G specifically shows variability in rendering multiple concepts—occasionally misplacing elements of the Ironman suit on a dog or failing to include it altogether. This phenomenon suggests that λ-*ECLIPSE* minimizes image diversity to enhance result consistency, a trait observed across the UnCLIP model family.

Figure 10 offers qualitative insights into the performance of λ-*ECLIPSE* without and with minimal fine-tuning. It is evident that in certain edge cases, where λ-*ECLIPSE* initially struggles to fully grasp novel visual concepts without finetuning, a modest application of few optimization iterations significantly enhances concept capture. Further optimization not only preserves text composition but also

enriches minor, subject-specific details, underscoring the adaptability and finesse of λ-*ECLIPSE* in nuanced image generation.

Moreover, in our evaluations using the Multibench dataset, we noticed that both the baseline models (Kosmos-G and Emu2) and λ-*ECLIPSE* encounter difficulties in precisely maintaining all subject-specific details, as depicted in Figure 14. **This underscores that zero-shot multi-subject P-T2I generation remains a significant challenge in the field.** Further, we explored how well each model preserves genuine human facial characteristics in various scenarios, particularly when combined with differing captions. The qualitative examples in Figure 13 shed light on this aspect. Although each model strives to maintain the original facial features, none succeeds in replicating the specific personal facial details accurately. These instances typically fall short of precisely conveying the intended compositions, with the exception of one scenario in IP-Adapter FaceID, indicating a notable area for future improvements in model performance.

H Limitations

Our work marks a pioneering venture into leveraging the latent space of pre-trained CLIP models for P-T2I generation. Nonetheless, it's crucial to recognize certain constraints. Primarily, despite its strengths, CLIP's inability to perfectly capture hierarchical representations occasionally leads to less-than-ideal results. This issue, stemming from the CLIP contrastive loss, can cause deviations from the original subject features, particularly when generating P-T2I for complex subjects like human faces. We believe that enhancing CLIP's representations could significantly boost our framework's efficacy in P-T2I mapping. The λ-*ECLIPSE* model, trained on 34 million parameters and 1.6 million images, presents a substantial foundation. Yet, there's potential for further refinement, as increasing the quality of data and the number of parameters could yield even better outcomes.

I Broader Impact

Subject-driven image generation or Personalized Text-to-Image (P-T2I) methods have the potential to be a transformative tool in numerous domains. For their positive influence, they enable users to effortlessly generate, modify, and synthesize original subjects into diverse environments, thereby enriching creative expression. On the other hand, the ease of altering and creating images raises concerns about the responsible use of this technology which requires significant ethical and legal considerations. Users must be acutely aware of being able to infringe intellectual property rights and create misleading or harmful content. We recommend developers provide a more secure way such as image attribution [18] for end-users to ensure accountability for misuse of such models. As such, those employing subject-driven image-generation techniques should exercise careful judgment, ensuring that their work adheres to ethical standards and legal boundaries. It is imperative that the broader implications of this technology are considered, and that a commitment to responsible and conscientious use guides its application.

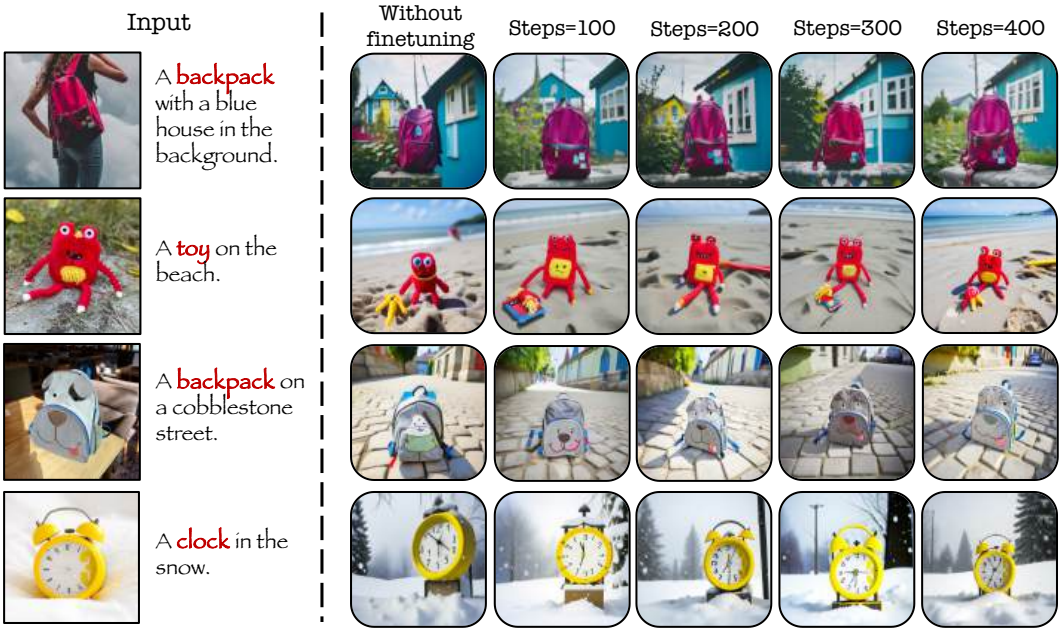

Figure 10: Qualitative examples of λ-*ECLIPSE* without finetuning and different stages of finetuning.

Figure 11: Qualitative examples of the increasing complexity of novel visual concepts as we move from top to bottom.

Figure 12: Qualitative examples of showcasing the consistency comparisons between Kosmos-G and λ-*ECLIPSE*.

Figure 13: Qualitative examples of showcasing the failure cases on human faces on Kosmos-G, IP-Adapter (SDXL), IP-Adapter (FaceID), and λ-*ECLIPSE*.

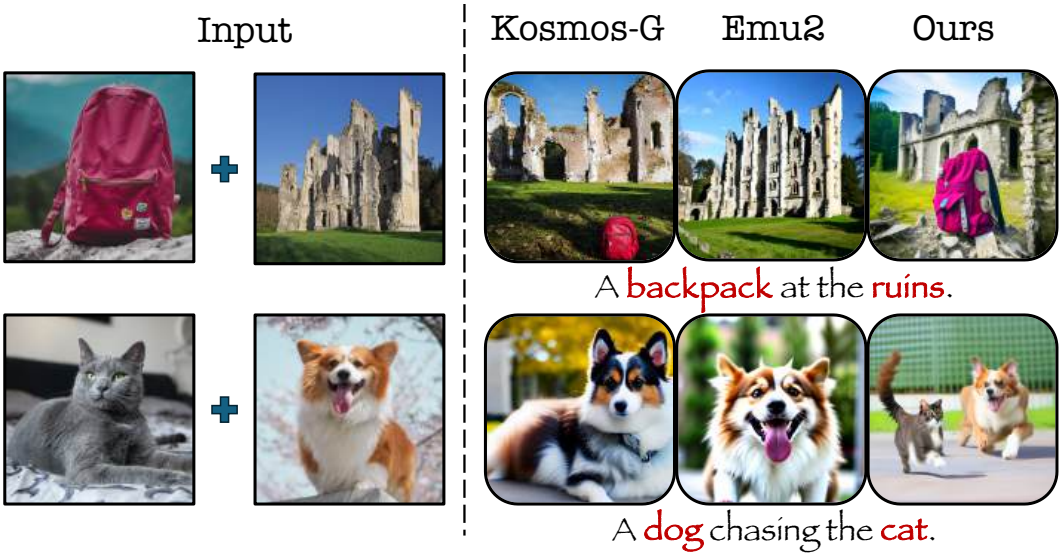

Figure 14: Qualitative examples of showcasing the failure cases on Multibench of Kosmos-G, Emu2, and λ-*ECLIPSE*.